

MODELLING SPIRAL PHYLLOTAXIS

DEBORAH R. FOWLER, JAMES HANAN, and PRZEMYSŁAW PRUSINKIEWICZ
Department of Computer Science, University of Regina, Regina, Saskatchewan, Canada S4S 0A2

Abstract—In this paper, established geometric models of phyllotaxis are used to generate realistic images of flowers and fruits with spiral patterns. Two approaches to the placement of organs are considered: spiral arrangement on a plane and spiral arrangement on the surface of a cylinder. Images of sunflowers, daisies and zinnias have been synthesized using the planar model, while the cylindrical model is illustrated by pine cones and a pineapple.

1. INTRODUCTION

The term *phyllotaxis* means leaf arrangement; however, it is more generally used to denote the regular arrangement of lateral organs (leaves on a stem, cone scales on a cone axis, florets in a composite flower head) observed in most higher plants. Thus, spiral phyllotaxis refers to those arrangements which exhibit spiral patterns. The extensive literature generated by biologists' and mathematicians' interest in phyllotaxis is reviewed by Erickson[3] and Jean[6]. The proposed models range widely from purely geometric descriptions (for example, Coxeter[2]) to complex physiological hypotheses tested by computer simulations (Hellendoorn and Lindenmayer[5], Veen and Lindenmayer[12], Young[14]). This paper applies two existing models to synthesize realistic images of flowers and fruits which exhibit spiral phyllotactic patterns.

Both models relate phyllotaxis to packing problems. The first one operates in a plane and was originally proposed by Vogel[13] to describe the structure of a sunflower head. A further detailed analysis was given by Ridley[9, 10]. The second model reduces phyllotaxis to the problem of packing circles on the surface of a cylinder. Its analysis was presented by van Iterson[11] and extensively reviewed by Erickson[3].

The mathematical models of phyllotaxis describe relative positions of organs, but are not concerned with their exact shapes. However, even when the component organs are relatively small, their individual appearance must be adequately modelled to produce a realistic synthetic image. The proposed approach is to represent each organ (such as a single floret or a petal) using a bicubic surface consisting of one or more patches. The exact surface shape is defined interactively with a graphical patch editor. A phyllotaxis model is then applied to assemble the predefined surfaces into a final structure. During this process, the surfaces are translated and rotated in two or three dimensions until they reach their target positions; in some cases the required transformations also include scaling. In order to prevent excessive regularity, several variations of a particular shape may be incorporated in a given structure.

A related approach to the placement of organs was proposed by Prusinkiewicz[7] and Hanan[4] for incorporating leaves and flowers into developmental models of plants expressed in terms of L-systems. Many examples are presented by Prusinkiewicz, Lindenmayer

and Hanan[8]. In contrast, the present paper employs phyllotactic models. As a result, much more intricate spiral patterns can be obtained.

The area of phyllotaxis is dominated by intriguing mathematical relationships. One of them is the "remarkable fact that the numbers of spirals which can be traced through a phyllotactic pattern are predominantly integers of the Fibonacci sequence" [3, p. 54]. For example, Coxeter[2] notes that the pineapple displays 8 rows of scales sloping to the left and 13 rows sloping to the right. Furthermore, it is known[2] that the ratios of consecutive Fibonacci numbers F_{k+1}/F_k converge towards the golden mean $\tau = (\sqrt{5} + 1)/2$. The Fibonacci angle $360^\circ \tau^{-2}$, approximately equal to 137.5° , is the key to the first model discussed.

2. THE PLANAR MODEL

In order to describe the pattern of florets (or seeds) in a sunflower head, Vogel[13] proposed the following formula:

$$\phi = n * 137.5^\circ \quad r = c\sqrt{n}$$

where

- n is the ordering number of a floret, counting outward from the center; it is the reverse order of floret age in a real plant.
- ϕ is the angle between a reference direction and the position vector of the n^{th} floret in a polar coordinate system originating at the center of the capitulum. It follows that the *divergence angle* between the position vectors of any two successive florets is constant, $\alpha = 137.5^\circ$, as illustrated in Fig. 1.
- r is the distance between the center of the capitulum and the center of the n^{th} floret, given a constant scaling parameter c .

The square-root relationship between the distance r and the floret ordering number n has a simple geometric explanation. Assuming that all florets have the same size and are densely packed, the total number of florets which fit inside a disc of radius r is proportional to the disk area. Thus, the ordering number n of the most extremely positioned floret in the capitulum is proportional to r^2 , or $r \sim \sqrt{n}$.

The divergence angle of 137.5° is much more dif-

difficult to explain. Vogel[13] derives it using two assumptions:

- Each new floret is issued at a fixed angle α with respect to the preceding floret;
- The position vector of each new floret fits into the largest existing gap between the position vectors of the older florets.

Ridley[9] does not object to these basic assumptions, but indicates that they are insufficient to justify the occurrence of the Fibonacci angle, and points to several arbitrary steps present in Vogel's derivation. Ridley's own explanations proceed in two directions. In the paper[9] he shows that if Vogel's formula is parameterized:

$$\phi = n * \alpha \quad r = c\sqrt{n},$$

an appropriately defined packing efficiency of equal-area elements reaches a maximum for $\alpha = 137.5^\circ$. From this perspective, the distribution of florets reflects a plant's attempt to place the maximum number of florets in a head of a given size. A computer simulation explaining a causal mechanism by which this pattern may be produced is presented in [10]. The underlying concept that florets move and take final positions in response to the pressure they exert on one another was originally advanced by Adler[1].

Ridley[9] points out that although a comprehensive justification of Vogel's formula may require further research, the model correctly describes the arrangement of florets visible in actual composite capitula. The most prominent feature is two sets of spirals or *parastichies*, one turning clockwise, the other counterclockwise, which are composed of nearest neighbouring florets. The number of spirals in each set is always a member of the Fibonacci sequence; 21 and 34 for a small capitulum, up to 89 and 144 or even 144 and 233 for large ones. For example, in the image of a domestic sunflower capitulum (Fig. 2), one can discern 34 spirals running clockwise and 55 spirals running counterclockwise. The number of perceived spirals depends on the capitulum size expressed in terms of the number of component florets. If one limits their field of attention to a circle approximately 2/3 the size of the entire sunflower capitulum in Fig. 2, the number of discernible spirals becomes 21 and 34. The capitulum of a daisy (Fig. 3) also exhibits 34 clockwise spirals and 21 counterclockwise spirals.

A complete model of a flower head, suitable for realistic image synthesis, should contain several organs of various shapes. This is easily achieved by associating different surfaces with specific ranges of the index n . Additionally, a random selection of similar surfaces can be employed to prevent excessive regularity of the resulting image. Other extensions to the basic model consist of varying organ orientation in space and changing their altitude from the plane of the head as a function of n . For example, the dipped central portion of the daisy (Fig. 3) was obtained by lowering the position of the first several florets. By changing the shape

and colour of surfaces and adjusting the few parameters mentioned above, other types of flowers can be generated using the same underlying model. This is illustrated by the figures of common sunflowers (Fig. 4) and zinnias (Fig. 5).

Fig. 4 includes flowers in four developmental stages: buds, young flowers starting to open, open flowers and older flowers where the petals begin to droop. All flowers are generated using approximately the same number of florets. The central florets are represented by the same surface at each stage. The surfaces representing petals and their orientation vary from one stage to another. The relative sizing of the flowers was achieved by scaling after the flowers were created.

The zinnias (Fig. 5) illustrate the effect of changing a petal's altitude, size and orientation as a function of n . The height at which a petal is placed decreases by a small amount as n increases. The size of each successive petal is incremented linearly. The orientation is also adjusted linearly by a small angle increment. Thus, the petals with small values of index n are placed more vertically, while the petals with larger indices n are more horizontal.

3. THE CYLINDRICAL MODEL

The spiral patterns evident in elongated organs such as pine cones, fir cones and pineapples, can be described by models which position components, in this case scales, on the surface of a cylinder. van Iterson[11] divides phyllotactic patterns on cylinders into *simple* and *conjugate* ones. In the case of a simple arrangement, all components lie on a single *generative helix*. In contrast, conjugate patterns consist of two or more interleaved helices. This paper discusses simple phyllotactic patterns only. They are generally characterized by the following formula:

$$\phi = n * \alpha \quad r = \text{const} \quad H = h * n \quad (1)$$

where

- ϕ , r and H are the cylindrical coordinates of scale n ;
- n is the ordering number of a scale, counting from the bottom of the cylinder;
- α is the divergence angle between two consecutive scales; as in the planar case, it is assumed to be constant;
- h is the vertical distance between two consecutive scales (measured along the main axis of the cylinder).

In the planar model, the constant divergence angle $\alpha = 137.5^\circ$ is found across a large variety of flower heads. The number of perceived parastichies is determined by the capitulum size, and it changes as the distance from the capitulum center increases. In contrast, a phyllotactic pattern on the surface of a cylinder is uniform along the entire cylinder length. The number of evident parastichies depends on the values of parameters α and h . The key problem, both from the viewpoint of understanding the geometry of the pattern and applying it to generate synthetic images, is to express the divergence angle α and the vertical displace-

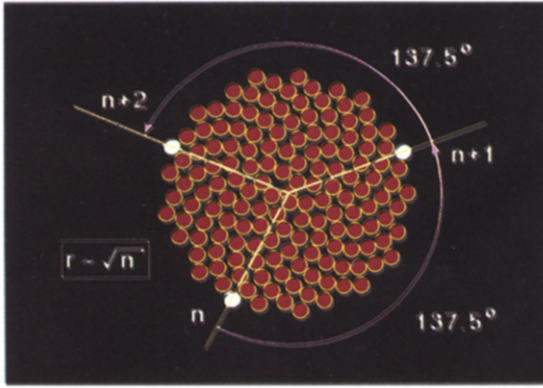


Fig. 1. Pattern of florets in a sunflower head, according to Vogel's formula.



Fig. 4. Common sunflowers.



Fig. 2. Domestic sunflower head.



Fig. 5. Zinnias.

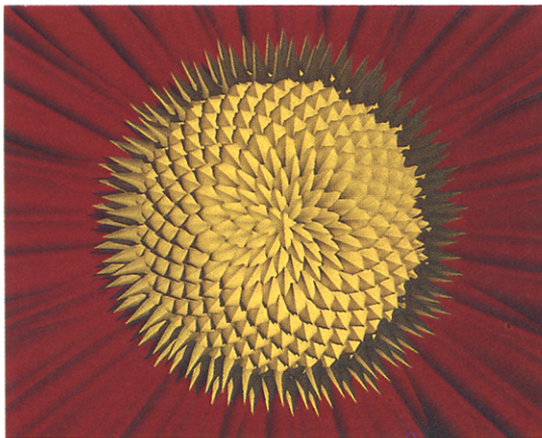


Fig. 3. Close-up of a daisy capitulum.

ment h as a function of the numbers of evident parastichies encircling the cylinder in the clockwise and counterclockwise directions. A solution to this problem was proposed by van Iterson [11] and reviewed by Erickson [3]. Our presentation closely follows that of Erickson.

The phyllotactic pattern can be explained in terms of circles packed on the surface of the cylinder. An evident parastichy consists of a sequence of tangent circles, the ordering numbers of which form an arithmetic sequence with difference m . The number m is referred to as the *parastichy order*. Thus, the circles on the cylinder surface may be arranged in two congruent 2-parastichies, five congruent 5-parastichies, etc. The angular displacement between two consecutive circles in an m -parastichy is denoted by δ_m . By definition, δ_m belongs to the range $(-\pi, \pi]$ radians. The relation between the angular displacement δ_m and the divergence angle α is expressed by the formula:

$$\delta_m = m\alpha - \Delta_m 2\pi \tag{2}$$

where Δ_m is an integer which van Iterson calls the *encyclic number*. It is the number of turns around the cylinder, rounded upward or downward to the nearest integer, which the generative helix describes between two consecutive points of the m -parastichy.

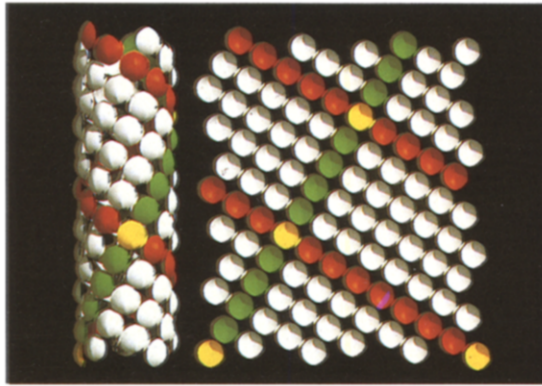


Fig. 6. Parastichies on the surface of a cylinder and on the unrolled cylinder. A 5-parastichy is shown by red disks and an 8-parastichy by green disks. Yellow disks are common to both parastichies. Disk number 0 (bottom left) is repeated on the right side of the unrolled cylinder (as in Erickson[3, Fig. 3.1]).

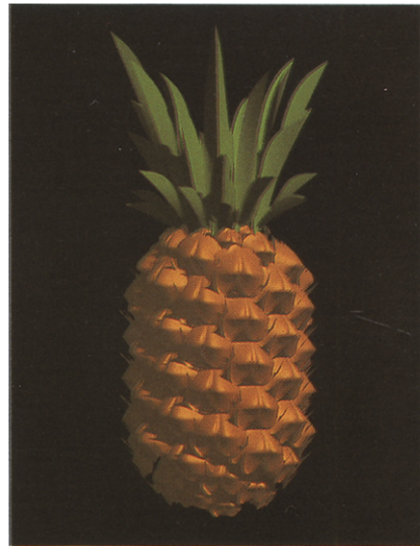


Fig. 9. A pineapple.

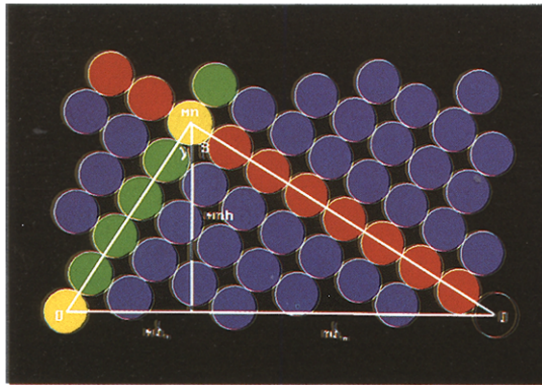


Fig. 7. An opposite parastichy triangle. The base is formed by the circumference of the cylinder. The other two sides are formed by the parastichies (as in Erickson[3, Fig. 3.8]).



Fig. 10. Pine cones.

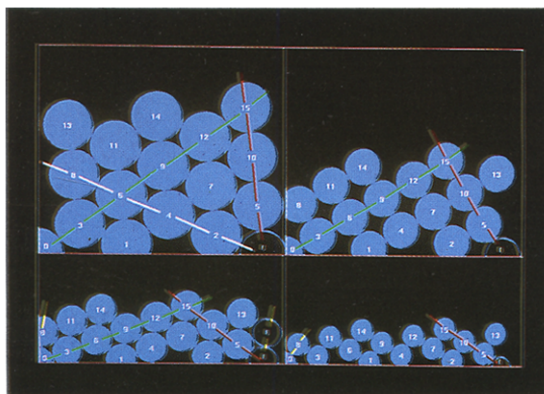


Fig. 8. Patterns of tangent circles drawn on the surface of a cylinder as a function of circle diameter. Top left: Each circle has six tangent circles; 2, 3 and 5-parastichies can be discerned. Top right: As the circle diameter decreases, the 2-parastichy disappears. Bottom left: as the circle diameter decreases even further, an 8-parastichy is formed. Bottom right: the 3-parastichy disappears (as in Erickson[3, Fig. 3.9]).

Usually, one can perceive two series of parastichies running in opposite directions (Fig. 6). The second parastichy satisfies an equation analogous to (2):

$$\delta_n = n\alpha - \Delta_n 2\pi. \tag{3}$$

Consider the m - and n -parastichies starting at the circle 0. In their paths across the cylinder, they will intersect again at the circle mn . Assume that m and n are relatively prime; otherwise the phyllotactic pattern would have to contain several circles lying at the same height H and, contrary to the initial assumption, would not be simple. Thus, the circle mn is the first point of intersection between the m -parastichy and the n -parastichy above circle 0. Consequently, the path from circle 0 to mn along the m -parastichy, and back to 0 along the n -parastichy, encircles the cylinder exactly once. The section of m -parastichy between circles 0 and mn consists of $n + 1$ circles (including the endpoints), so the angular distance between the circles 0 and mn is equal to $n\delta_m$. Similarly, the distance between circles 0

and mn measured along the n -parastichy can be expressed as $m\delta_n$. As a result:

$$n\delta_m - m\delta_n = \pm 2\pi. \quad (4)$$

The signs in the above equation correspond to the assumption that the spirals encircle the cylinder in opposite directions; thus one of the values δ is positive and the other one is negative. Substituting the right sides of Eqns. (2) and (3) for δ_m and δ_n yields:

$$n\Delta_m - m\Delta_n = \pm 1. \quad (5)$$

To further analyze the pertinent geometric relationships, cut the cylinder along the vertical line passing through the center of circle 0, and "unroll" the resulting surface (Fig. 6). The two parastichies and the circumference of the cylinder passing through point 0 form a triangle as shown in Fig. 7. The perpendicular to the base from point mn divides this triangle into two right triangles. If d denotes the diameter of the circles, then:

$$(n\delta_m)^2 + (mnh)^2 = (nd)^2, \quad (6)$$

and

$$(m\delta_n)^2 + (mnh)^2 = (md)^2. \quad (7)$$

The above system of equations can be solved with respect to h and d :

$$h = \sqrt{(\delta_m^2 - \delta_n^2)/(n^2 - m^2)}, \quad (8)$$

$$d = \sqrt{(n^2\delta_m^2 - m^2\delta_n^2)/(n^2 - m^2)}, \quad (9)$$

or, taking into consideration Eq. (4),

$$d = \sqrt{2\pi(n\delta_m + m\delta_n)/(n^2 - m^2)}. \quad (10)$$

Now, the problem is to determine values of δ_m and δ_n . They are not simply functions of parameters m and n . Fig. 8 shows that, for given m and n , the values of δ_m and δ_n can be chosen from a certain range, yielding parastichies which are of differing steepness. In order to determine this range, observe that at each range limit a change of phyllotactic pattern occurs: one previously evident parastichy disappears, and another is formed. Thus, at the range limit *three* evident parastichies coexist. It follows from Fig. 8 that at one end of the range the third parastichy has order $|m - n|$, and at the other end it is an $(m + n)$ -parastichy. Furthermore, three coexisting parastichies imply that each circle is tangent to six other circles, as seen on the left of the diagram, or all circles lie in the vertices of a regular hexagonal grid, as seen on the right. Consequently, the angle $\beta + \gamma$ at vertex mn (Fig. 7) is equal to $2\pi/3$. Expressing the base of the triangle in terms of its two sides and their included angle results in:

$$(2\pi)^2 = (nd)^2 + (md)^2 - 2(nd)(md)\cos(2\pi/3), \quad (11)$$

or, after simplification,

$$d = 2\pi/\sqrt{m^2 + mn + n^2}. \quad (12)$$

A comparison of Eqns. (12) and (10) yields:

$$n\delta_m + m\delta_n = 2\pi(n^2 - m^2)/(m^2 + mn + n^2). \quad (13)$$

Solving the system of Eqns. (4) and (13) with respect to δ_m and δ_n produces:

$$\delta_m = \pi(m + 2n)/(m^2 + mn + n^2), \quad (14)$$

$$\delta_n = \pi(2m + n)/(m^2 + mn + n^2). \quad (15)$$

Given the values of δ_m and δ_n , the divergence angle α can be found from either one of the Eqns. (2) or (3), assuming that the encyclic numbers Δ_m or Δ_n are known. From the definition of encyclic numbers, it follows that they are the *smallest* positive integers satisfying Eq. (5). A systematic method for solving this equation, based on the theory of continuous fractions, is presented by van Iterson[11]. Erickson[3] points out that in practice the solution can often be found by guessing. Another possibility is to look for the smallest pair of numbers (Δ_m, Δ_n) satisfying (5) using a simple computer program.

In summary, a phyllotactic pattern characterized by a pair of numbers (m, n) can be constructed as follows:

1. Find Δ_m and Δ_n from Eq. (5).
2. Find the range of admissible values of the angular displacements δ_m and δ_n . The limits can be obtained from Eqns. (14) and (15) using the originally given values of m and n for one limit, and the pair $(\min\{m, n\}, |m - n|)$ for the other.
3. For a chosen pair of admissible displacement values δ_m and δ_n , calculate the divergence angle α from Eq. (2) or (3) and the vertical displacement h from Eq. (8).
4. Find the diameter d of the circles from Eq. (9).

The diameter d does not enter directly in any formula used for image synthesis, but serves as an estimate of the size of surfaces to be incorporated in the model. As in the case of the planar model (Section 2), their exact shapes are defined interactively using a surface editor.

Fruit images synthesized using the cylindrical model are shown in Figs. 9 and 10. The pineapple (Fig. 9) is an example of a pattern where a given scale has six neighbours, which belong to 5, 8 and 13-parastichies. The corresponding divergence angle α is equal to 138.1395° . The pine cones (Fig. 10) were generated using the values $m = 5$, $n = 8$ and $\alpha = 137.5^\circ$ (the divergence angle α for a (5, 8)-parastichy pattern must belong to the interval from 135.9184° to 138.1395°). From these values, h and d were calculated as a function

of the radius of the cylinder. The effect of closing the bottom and top of the pineapple and pine cones was achieved by decreasing the diameter of the cylinder and the size of the scales.

4. CONCLUSIONS

In this paper, two models of phyllotactic patterns have been applied to create realistic images of plant organs. The first model describes phyllotaxis on a plane and is particularly suitable to generate images of composite flowers, such as sunflowers and daisies. The second model operates on the surface of a cylinder and provides a convenient approach to the synthesis of elongated organs with spiral patterns, for example pineapples and pine cones. The shapes of the component elements, such as florets, scales or seeds, are defined interactively using a parametric surface editor.

One problem open for further research is related to the modelling of organ parts the shape of which cannot be approximated adequately by disks or cylinders. For example, the diameter of a pineapple and a pine cone decreases at the base and at the top of the fruits. The mathematical model of phyllotaxis on a cylinder does not take this effect into account. The gradual decrease of the diameter of the cylinder and the size of the scales does not produce fully satisfactory results.

Another problem is related to collisions between elements of the modelled objects. For example, it would be difficult to avoid intersections between the tightly packed surfaces representing petals of roses or peonies.

Acknowledgements—Our interest in phyllotactic patterns was inspired by Aristid Lindenmayer, who suggested simulations using Vogel's formula and provided the initial guidance through the literature on the subject. Figs. 2, 3, 5, 6 and 10 were rendered using the ray-tracer *rayshade* written by Craig Kolb. The generous support of the Department of Computer Science, University of Regina, and the Natural Sciences and Engineering Research Council of Canada is gratefully ac-

knowledged. The third author also wishes to thank Benoit Mandelbrot and the Department of Computer Science at Yale University for their support during completion of this paper.

REFERENCES

1. I. Adler, A model of contact pressure in phyllotaxis. *J. Theoret. Biol.* **45**, 1–79 (1974).
2. H. S. M. Coxeter, *Introduction to Geometry*. John Wiley & Sons, New York (1961).
3. R. O. Erickson, The geometry of phyllotaxis. In J. E. Dale and M. L. Milthorpe (Eds.), *The Growth and Functioning of Leaves*. Cambridge University Press, Cambridge, MA, pp. 53–88 (1983).
4. J. Hanan, Plantworks: A software system for realistic plant modelling, M.Sc. Thesis, University of Regina, Saskatchewan, Canada (November 1988).
5. P. H. Hellendoorn and A. Lindenmayer, Phyllotaxis in *Bryophyllum tubiflorum*: Morphogenetic studies and computer simulations. *Acta Botanica Neerlandica* **23**, 473–92 (1974).
6. R. V. Jean, Mathematical modeling in phyllotaxis: The state of the art. *Mathematical Biosciences* **64**, 1–27 (1983).
7. P. Prusinkiewicz, Applications of L-systems to computer imagery. In H. Ehrig *et al.* (Eds.), *Graph Grammars and Their Application to Computer Science; Third International Workshop*. Lecture Notes in Computer Science **291**, Springer-Verlag, Berlin, pp. 534–548 (1987).
8. P. Prusinkiewicz, A. Lindenmayer, and J. Hanan, Developmental models of herbaceous plants for computer imagery purposes, Proceedings of SIGGRAPH '88 (Atlanta, Georgia, August 1–5, 1988). In *Comp. Graphics* **22**(4), 141–150 (1988).
9. J. N. Ridley, Packing efficiency in sunflower heads. *Mathematical Biosciences* **58**, 129–139 (1982).
10. J. N. Ridley, Computer simulation of contact pressure in capitula. *J. Theoret. Biol.* **95**, 1–11 (1982).
11. G. van Iterson, *Mathematische und mikroskopisch-anatomische Studien über Blattstellungen*. Gustav Fischer, Jena (1907).
12. A. H. Veen and A. Lindenmayer, Diffusion mechanism for phyllotaxis, theoretical, physico-chemical and computer study. *Plant Physiology* **60**, 127–139 (1977).
13. H. Vogel, A better way to construct the sunflower head. *Mathematical Bioscience* **44**, 179–189 (1979).
14. D. A. Young, On the diffusion theory of phyllotaxis. *J. Theoret. Biol.* **71**, 421–423 (1978).